A STUDY OF PHASE TRANSITIONS IN SODIUM STEARATE BY MEANS OF NUCLEAR MAGNETIC RESONANCE

BY

ROWLAND FREDERICK GRANT

A thesis submitted in partial fulfilment of the requirements for the degree of Master of Science in Chemistry.

We accept this thesis as conforming to the standard required from candidates for the degree of Master of Science

Members of the Department
of Chemistry

THE UNIVERSITY OF BRITISH COLUMBIA
October, 1955.

ABSTRACT

The mesomorphic phase transitions of sodium stearate occurring between 23°C. and 200°C. were investigated by means of the nuclear magnetic resonance of the hydrogen nuclei in sodium stearate. The changes in the nuclear magnetic resonance line width as the temperature increased revealed three phase transitions. These are the supercurd-subwaxy transition at 114°C., the subwaxy-waxy at 130°C., and the waxy-superwaxy transition at approximately 165°C.. Since the nuclear magnetic resonance line width is reduced as molecular motion increases, a general explanation of the phase transitions has been attempted.

Stearic acid was also investigated by means of nuclear magnetic resonance at temperatures between 24°C. and 90°C.. Only one transition, the melting point at 70°C. could be detected.

ACKNOWLEDGMENTS

I am indebted to Dr. B. A. Dunell for guiding this research and for taking a constant interest in the work. I am grateful to Dr. G. M. Volkoff who kindly supplied much of the apparatus used in this research and who also supplied a place to work among his students in the Physics building.

I would also like to thank Mr. H. A. Buckmaster and Mr. R. R. Haering for many stimulating discussions. I am particularly indebted to Mr. N. Hedgecock for his aid in solving technical problems and to my brother Alan for his assistance in drawing some of the diagrams and checking some of the results.

The support of the National Research Council in the form of a research grant to Dr. Dunell is gratefully acknowledged.

TABLE OF CONTENTS

	Page No.
CHAPTER I INTRODUCTION	
A. Fatty Acid Salts	
Phase Transitions in Sodium Stearate	1
Hydrated Forms of Sodium Stearate	2
Mechanisms of the Phase Transitions	3
B. Nuclear Magnetic Resonance	
Fundamental Background	4
Relaxation Times	7
Application to Solid State Problems	8
CHAPTER II APPARATUS	
General Description	10
Arrangement of the Apparatus	11
The Oscillating Detector	12
The Thermostat	14
CHAPTER III EXPERIMENTAL	
A. Methods	
Preparation of Sodium Stearate	16
Operation of the Thermostat	17
Measurement of Resonance Absorption	18
Sources of Error	18
B. Results	
Phase Transitions in Sodium Stearate	19
An Investigation of Stearic Acid	21
Line Shapes of Sodium Stearate	21

Page No.

CHAPTER IV DISCUSSION

Stearic Acid 22

Sodium Stearate 22

Interpretation of a Line Shape of Sodium Stearate 24

Future Work 25

APPENDIX

Line Widths of Sodium Stearate Used in Figure 9 26

REFERENCES 27-28

LIST OF ILLUSTRATIONS

		Facing Page
Figure 1	Block Diagram of the Apparatus	11
Figure 2	The Livingston Oscillating Detector and Audio Amplifier	13
Figure 3	Photograph of the Livingston Oscillating Detector and Audio Amplifier	13
Figure 4	The Regenerative Oscillating Detector and Audio Amplifier	14
Figure 5	Photograph of the Regenerative Oscillating Detector and Audio Amplifier	14
Figure 6	Modified Regenerative Oscillating Detector	14
Figure 7	The Experimental Arrangement	15
Figure 8	Line Width Change in Sodium Stearate as the Sample Cools	19
Figure 9	Line Width Change in Sodium Stearate as Temperature is Raised	20
Figure 10	Line Width Change in Stearic Acid as Temperature is Raised	21
Figure 11	Resonance Absorption Line Shapes in Sodium Stearate	21

CHAPTER 1 INTRODUCTION

A. Fatty Acid Salts.

Phase Transitions in Sodium Stearate.

Soaps of fatty acids containing more than four carbon atoms exhibit mesomorphism(36). On heating they pass through a series of transitions before melting into isotropic liquids. Fatty acid soaps are geometrically anisotropic and have only one strongly polar group. Such properties generally favour the formation of mesomorphic phases(4). Some of these transitions show themselves as sharp changes in appearance which are most striking when observed between the crossed nichols of a polarizing microscope. The temperature of a transition is usually determined experimentally by measuring a property such as electrical conductivity(35), density(31)(27), thermal capacity(8) or viscosity(20)(26) as the temperature varies. The transition temperature appears as a change of slope when the property observed is plotted against temperature. This general procedure has revealed several mesomorphic transitions in sodium stearate.

Anhydrous sodium stearate, $C_{17}H_{35}COONa$ is a white opaque solid which becomes suddenly translucent and plastic above 130°C., partly transparent above 200°C. and completely transparent above 265°C.(8). There are other phase transitions which are not easily found visually. The following is a list of all the phases so far observed in anhydrous sodium stearate. The range of temperature given for the beginning of each transition indicates the extent of the agreement existing among different workers using different methods.

Name of Transition	Transition Temperature	References
Genotypical Point	65-70 °C.	28,32,26
Curd to Supercurd	89-93 °C.	30,33
Supercurd to Subwaxy	110-117°C.	32,26
Subwaxy to Waxy	125-134°C.	3,32,33
Waxy to Superwaxy	165-167°C.	3,30,31
Superwaxy to Subneat	198-209°C.	27,30,31,32
Subneat to Neat	226-262°C.	27,30,31,32,35
MeltingPoint	278-290°C.	20,31,35

Hydrated Forms of Sodium Stearate.

Sodium stearate can exist in several hydrated forms. On crystallization from 95% ethanol, one molecule of sodium stearate combines with half a molecule of water producing the alpha form. When heated to 52°C. the beta form is obtained which has one eighth of a molecule of water per molecule of sodium stearate. If the alpha or beta forms are heated above 103°C. the gamma or anhydrous form results. These forms differ slightly in crystal structure and can be distinguished from one another best by X-ray analysis(6)(29)(34). There is at least one more form of sodium stearate in combination with water which is not a stoichiometric hydrate but may instead be a solid solution(34).

The anhydrous sodium stearate used for phase transition studies is usually obtained by melting the alpha form under vacuum to remove the water of hydration(17)(27). It has been suggested that this treatment may not be drastic enough to remove the last traces of water associated with the sodium ion(15), and some of the phase transitions reported might in some

manner be due to the water. However, sodium stearate prepared by reacting molten stearic acid with sodium amalgum under vacuum showed the same phases as the sample prepared by melting the alpha form[27]. Therefore, the phase transitions in sodium stearate are not due to the influence of small amounts of water. The explanation now given is that the phase transitions in anhydrous soaps occur as the intermolecular forces are overcome by molecular motion when the temperature increases[27].

Mechanism of the Phase Transitions.

X-ray analysis shows that soaps consist of layers of double molecules placed end to end, hydrocarbon to hydrocarbon and carboxyl group to carboxyl group[16]. The sodium carboxylic groups have strong polar bonds between them and the adjacent hydrocarbon chains are held together by weaker van der Waal's forces. In general, low temperature transitions are due to rearrangement of the hydrocarbon chains while at high temperatures there is a rearrangement of the polar ends of the molecules[33].

Stearic acid melts at 68.5°C.. It has been suggested that at this temperature the cohesional forces between the hydrocarbon parts of sodium stearate should be overcome. Sodium stearate does not melt at 68.5°C. however since the forces between the sodium carboxylate groups probably maintain the mean position of the hydrocarbon chains[9]. The genotypical point at 70°C. probably indicates that the thermal energy is large enough to loosen the lattice in one dimension[28]. The hydrocarbon chains may now vibrate in one dimension. The amplitude of vibration may increase up to the curd-supercurd transition at 90°C. where vibrations begin in a second dimension, and give rise to a skipping rope type of motion. No simple explanation has been offered for the supercurd-subwaxy transition around 117°C., but it

probably represents a suddenly less restricted mode of motion of the hydrocarbon chains. The soap becomes quite plastic at the subwaxy to waxy transition so possibly the hydrocarbon chains have attained maximum freedom of motion in two dimensions[9]. The results of X-ray analysis indicate that the sodium stearate chains attain complete freedom of rotation at 165°C., the waxy-superwaxy transition[7]. The superwaxy to subneat transition around 200°C. and the subneat to neat transition around 265°C. are taken to represent two stages of reorientation of the sodium carboxylate groups[8]. In the neighbourhood of 300°C. sodium stearate becomes an isotropic liquid indicating that the polar attraction in the molecule has been overcome[9].

In general, these explanations for the phase transitions in sodium stearate are probably correct. Little direct physical or chemical evidence, however, exists to support them. An effective method now exists which may show whether or not the explanation involving vibration and rotation is correct. This method is the use of nuclear magnetic resonance techniques.

B. Nuclear Magnetic Resonance.

Fundamental Background.

Many atomic nuclei have a magnetic moment due to the spin of the nucleus. A nucleus with a spin I has a magnetic moment μ of the following magnitude:

$$\mu = g\mu_0\sqrt{I(I+1)}$$

where μ_0 equals $eh/2MC$, which is the nuclear magneton, and g is the nuclear g factor, which will be defined later. In a manner analogous

to atomic spectra it has been shown that when the nuclear magnets are placed in an external magnetic field Ho there will be an interaction and a nucleus of spin I will have 2I+1 energy levels accessible to it. These levels are Zeeman levels with energy values defined by:

$$E = g\mu_o m H_o$$

where $m = I, I-1, I-2 \text{ ---- } -I$

and $\Delta m = \pm 1$ (18)

The ffequency associated with difference in energy of each level may be expressed as

$$\nu_o = g \frac{\mu_o}{h} H_o$$

This is called the Larmor frequency and in a field of say 10,000 gauss ν_o will be in the radio frequency range. The nuclear g factor serves to relate the Larmor frequency and the field Ho for a given nucleus. The expression $g \frac{\mu_o}{h}$ is called the gyromagnetic ratio.

If one subjects a sample containing nuclear magnets to a weak magnetic field placed perpendicular to Ho and oscillating at the Larmor frequency ν_o, then a nucleus in a lower Zeeman energy level may absorb a quantum of energy from the radiation field and make a transition to the next higher energy state. If the frequency of the radiation field is not near the Larmor frequency one expects no absorption hence the term resonance phenomenon. There is an equal probability for a nucleus to go to a higher or a lower energy level, so that if all the levels were equally populated no net change should be expected. However, it can be shown that the thermal energy possessed by a nucleus far exceeds the energy difference between levels. Because of collisions due to thermal agitation the system

of nuclear spin states comes into thermal equilibrium with its surroundings. The result is not an equal population in all the energy levels, instead there is a Boltzman distribution favouring the lower levels. The difference in population is very small. For hydrogen nuclei at room temperature, in a field of 20,000 gauss, there are one million and fourteen nuclei in the lower states compared to one million in the upper states. This small excess is responsible for the energy absorption which can be observed at resonance[18].

The excess nuclei in the lower levels give rise to a nuclear paramagnetic bulk susceptibility:

$$\chi_o = (N/3KT)\, g^2 \mu_o^2\, I(I+1)$$

Since at resonance the equilibrium distribution of the nuclei is disturbed, the susceptibility is altered. This provides the means for measuring the nuclear magnetic resonance[18]. The susceptibility is a complex number with a real component χ' and an imaginary component χ'' which is 90° out of phase hence:

$$\chi = \chi' - i\chi''$$

It can be shown that the energy absorbed by a nuclear spin system is proportional to χ'', the out of phase component of magnetic susceptibility[18].

Now, there will be a net absorption of energy due to the transition between levels as long as there remains a surplus of nuclei in the lower states. To fulfill this latter condition, the net energy gained by the nuclei must be lost to the surrounding environment in some manner. This reduces the life time of the nuclei in the upper states causing a reduction of Δt in the Heisenberg equation:

$$\Delta E \cdot \Delta t \simeq h$$

The reduction of Δt increases the uncertainty of E, the energy of the level and thereby serves to broaden the line width. Line broadening is usually discussed in terms of relaxation times rather than the broadening of energy levels(25).

Relaxation Times.

The relaxation time is the time required for the system of nuclear spins to come to equilibrium with the environment and arises from the following interactions. The first relaxation mechanism arises from interaction of the magnetic moments of the nuclear spins with oscillatory magnetic fields produced by molecular motion of the lattice. The lattice refers to all the sample except the nuclear spins(21). This first mechanism governs the time required for all but $1/e$ of the equilibrium excess number to reach the lower energy state and is generally referred to as T_1, the spin-lattice relaxation time or the thermal relaxation time(18).

The second relaxation mechanism is due to interaction with oscillatory and stationary magnetic fields due to neighbouring nuclei with magnetic moments. There is one kind of interaction which involves an exchange of energy between neighbouring spins, called spin-spin collision, with no energy entering or leaving the spin system. This spin-spin collision limits the lifetime of a spin state and leads through the Heisenberg uncertainty relation to an energy spread(18)(25).

A second kind of interaction mechanism involwes a local magnetic field H_L superimposed on Ho. This local field on any given nucleus is the resultant of the local fields produced by the static components of neighbouring magnetic dipoles. The resonant condition is then:

$$\nu_0 = g \frac{\mu_0}{h} (H_0 + H_L)$$

Since H_L depends on the orientation of all neighbours, the result is a dispersion of the magnetic fields and hence a spread of values of at different nuclei throughout the sample. The average field and resonance frequency is still Ho and ν_0. From the resultant broadening of energy levels

$$\Delta E = g \frac{\mu_0}{\hbar} H_L$$

a time T_2 may be defined:

$$T_2 = \hbar/\Delta E = \frac{\hbar^2}{g\mu_0}/H_L \; .$$

This time T_2 is called spin-spin relaxation time and the line broadening it represents is due to resulting deviations from an average field Ho due to neighbouring nuclei and also due to spin collisions. It follows then, that inhomogeneities in Ho due to irregularities in the magnet pole pieces will cause a similar line broadening(18)(25).

Application to Solid State Problems.

The intermuclear fields are expected to be of the order of a few gauss in magnitude. This gives rise to line broadening in some solids, and the width of this broadening would also be a few gauss in magnitude. A quantitative relation between sample structure and line width has been developed for a solid having a rigid lattice. This relation involves a quantity called the "second moment of the line shape". If the magnitude of the energy absorption occurring during a sweep through the resonance condition is plotted against the change in magnetic field H, or radio-frequency ν, and if in such a plot it has the value F(H) at field H, then the second moment of the absorption line $\langle \Delta H^2 \rangle_{AV}$ is defined as follows:

$$\langle \Delta H^2 \rangle_{AV} = \int_{-\infty}^{\infty} F(H) \cdot (H - H^*)^2 \, dH$$

where $F(H)$ is the line shape function at any value of the field H, and H^* is the value of H at the centre of the absorption line. The second moment can be derived from experimental data by finding the total area under a plot of $F(H)\cdot(H-H^*)^2$ against H[25]. This method has been simplified to some extent and in certain cases the variation of line width due to motion of the lattice can be accounted for, so that it is possible to predict the second moment for some molecules with reasonable accuracy[10][12].

As lattice motion increases the resonance line width is reduced by averaging out the internuclear fields. In the case of a nucleus residing in a freely rotating molecule, the rotational periods are much smaller than the times associated with the nuclear resonance. If as well, all orientations of the molecule are equally probable, the internuclear fields average out to zero so that an extremely narrow line results. In practice, the width of this line is limited by the homogeneity of the field Ho over the sample. Since the reduction of line width due to lattice vibration is much smaller than that caused by rotation of a group, a sudden change in the line width is more likely to be caused by group rotation[1][5][18][25]. The measurement of the proton line width of sodium stearate at different temperatures might aid in determining the mechanisms involved in the various mesomorphic phase changes exhibited by sodium stearate.

CHAPTER II APPARATUS

General Description.

The apparatus used for this experiment is a standard nuclear magnetic resonance spectrometer. It consists of a large static homogeneous magnetic field Ho in which a solenoidal coil is placed with its axis perpendicular to the large field Ho. The sample under investigation is placed inside this solenoidal coil. The coil itself is part of a parallel resonant circuit. Energy is supplied to this circuit from a constant current source which is a weakly oscillating oscillator. The frequency of the oscillator is slowly changed by varying the capacity of the condenser in the resonant circuit. As the frequency passes through the resonant frequency of the nuclei in the sample, radio frequency energy is absorbed from the coil, thereby decreasing the amplitude of the radio frequency voltage across it. This decrease in amplitude can, in principle, be observed by amplifying and rectifying the radio frequency voltage and recording the rectified voltage. In order to avoid D.C. amplification which would be necessary in such an arrangement to obtain an observable signal, the large static magnetic field is modulated slightly at a low audio frequency. As a result, the resonance frequency of the nuclei oscillates about the value determined by the large static field. As the frequency of the oscillator is swept slowly through resonance, the radio frequency voltage across the coil is modulated at this audio frequency. The modulated radio frequency voltage is amplified and detected in a linear detector giving the audio signal plus noise. This is amplified further and passed through a narrow band amplifier tuned to the modulation frequency which reduces the noise while passing the signal. The signal is passed through a phase

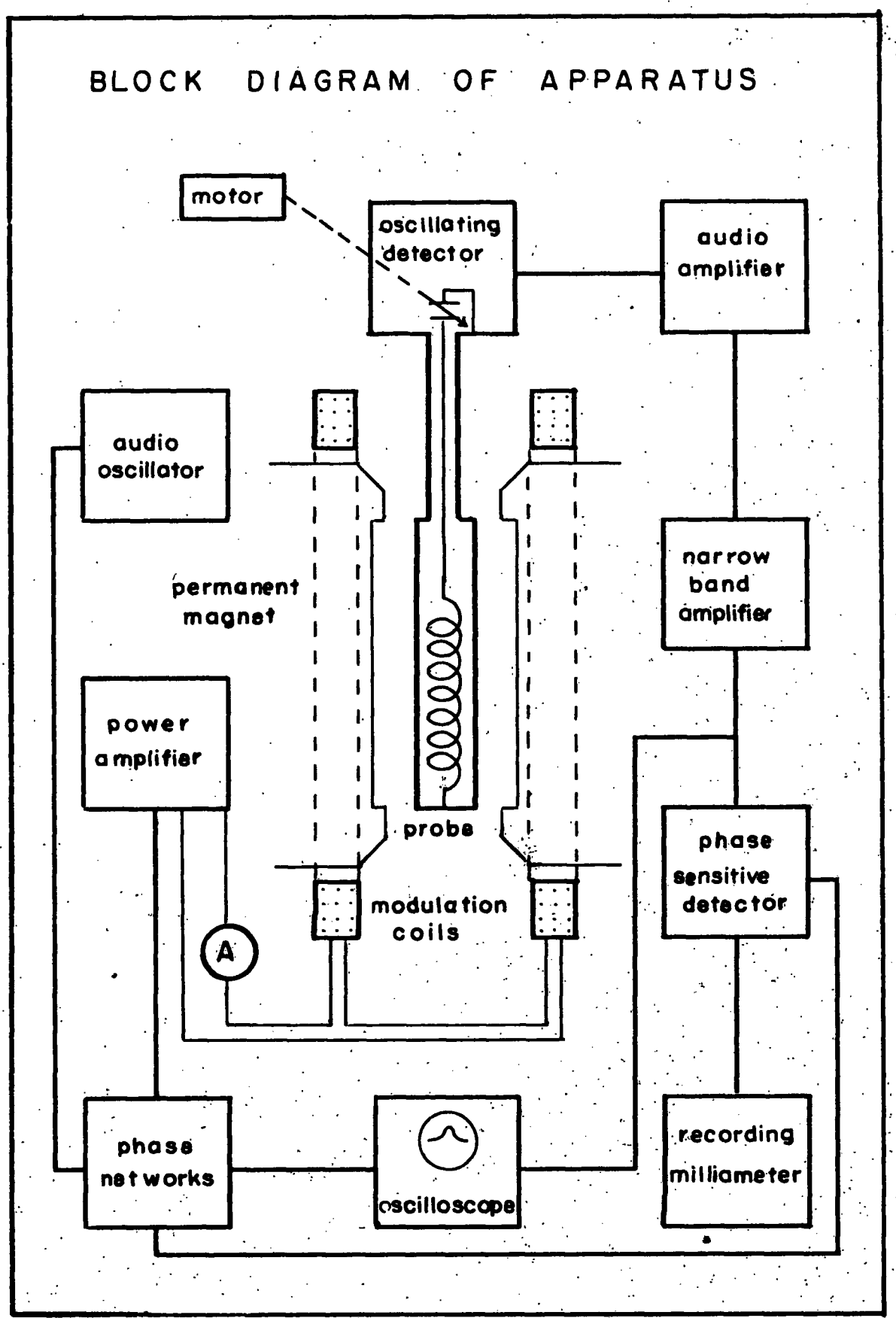

FIGURE I

TO FACE PAGE II

sensitive detector and on to a recording milliammeter. To decrease the noise present with the signal still further, a long time constant is included after the phase sensitive detector which narrows the band of the noise recorded. At the same time, the speed with which ~~data~~ results may be collected is limited by the fact that the time of sweeping through an absorption signal must be several times the time constant used, otherwise the circuit will not be able to follow the signal. If the modulation amplitude is less than one-third of the line width the recorded signal closely approximates the derivative of the absorption curve(37).

The Arrangement of the Nuclear Magnetic Resonance Spectrometer.

The arrangement of the nuclear magnetic resonance spectrometer is outlined by figure 1. The large permanent magnet was supplied by the Department of Physics of the University of British Columbia. The field of this magnet was measured as 7070 gauss at 24°C. throughout a gap 2.03 inches wide and 7.5 inches in diameter. Previous measurement has shown a field inhomogeneity of about 0.2 gauss in a volume of one cubic centimeter(37). The large static magnetic field was modulated by two Helmholtz coils wound on ten inch diameter bakelite forms and placed around the magnetic pole tips(37).

Some of the recording apparatus was also supplied by the Department of Physics. A Hewlett Packard Model 200B audio oscillator feeds a 30 cycle per second signal into the phase shift networks. The signal is amplified by a Williamson amplifier whose output drives the modulation coils(38). Another portion of the signal goes to the horizontal input of an Eico model 400 oscilloscope. A third part of the 30 cycles per

second signal is changed in phase by the phase shift networks and sent to the phase sensitive detector(24). The frequency of the oscillating detector is varied by a Gorrell and Gorrell type M adjustable drive motor. The 30 cycles per second audio component is amplified by a restricted band audio amplifier and is amplified again by a narrow band amplifier tuned to pass thirty cycles. The output of the narrow band amplifier goes to the vertical input of the oscilloscope and to the phase sensitive detector. The derivative of the nuclear magnetic resonance absorption signal is recorded by an Esterline Angus recording milliammeter(37).

The frequency of the oscillating detector was measured by mixing radiation from it with that from a Lampkin Type 105B frequency meter in an Eddystone Model 650 radio receiver. The output of the receiver was displayed on a small oscilloscope and when the beat frequency passed through zero a mark was made on the chart by momentarily shorting the side of the recorder to ground. The frequency at any point on the chart measured by interpolating between two frequency marks, assuming that the frequency varied linearily with distance along the chart(37).

The Oscillating Detector.

The oscillating detector is a modified Colpitts oscillator followed by an audio amplifier. The sample in the parallel resonance coil of the oscillator absorbs radio frequency energy. This changes the oscillation amplitude which changes the grid voltage of the oscillator tube. The change in grid voltage appears as an audio component at the modulation frequency in the plate voltage of the oscillator tube. The audio component is fed into the audio amplifier after the radio frequency component of the signal is bypassed. This system responds only to the absorptive component of

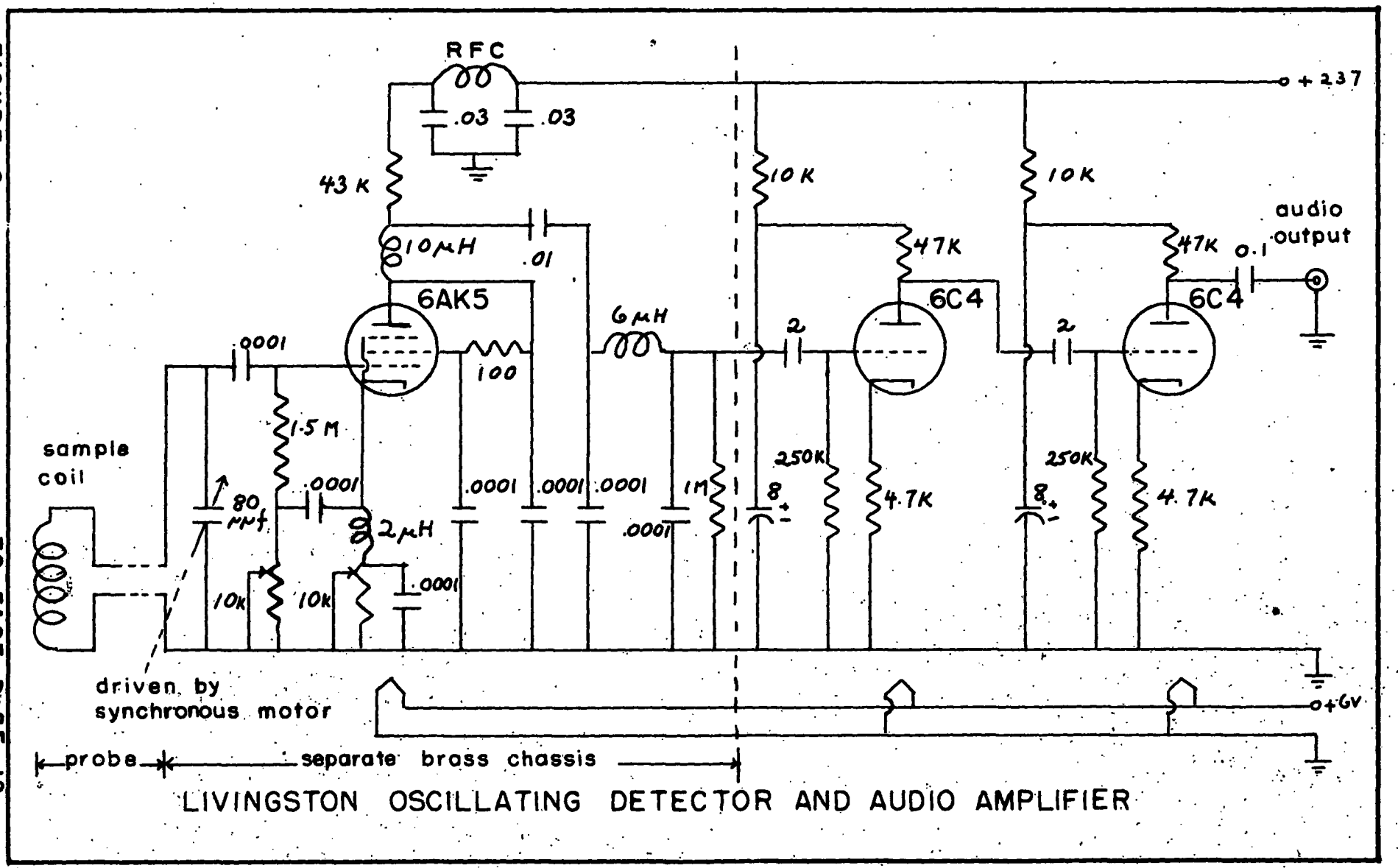

FIGURE 2

LIVINGSTON OSCILLATING DETECTOR AND AUDIO AMPLIFIER

TO FACE PAGE 13

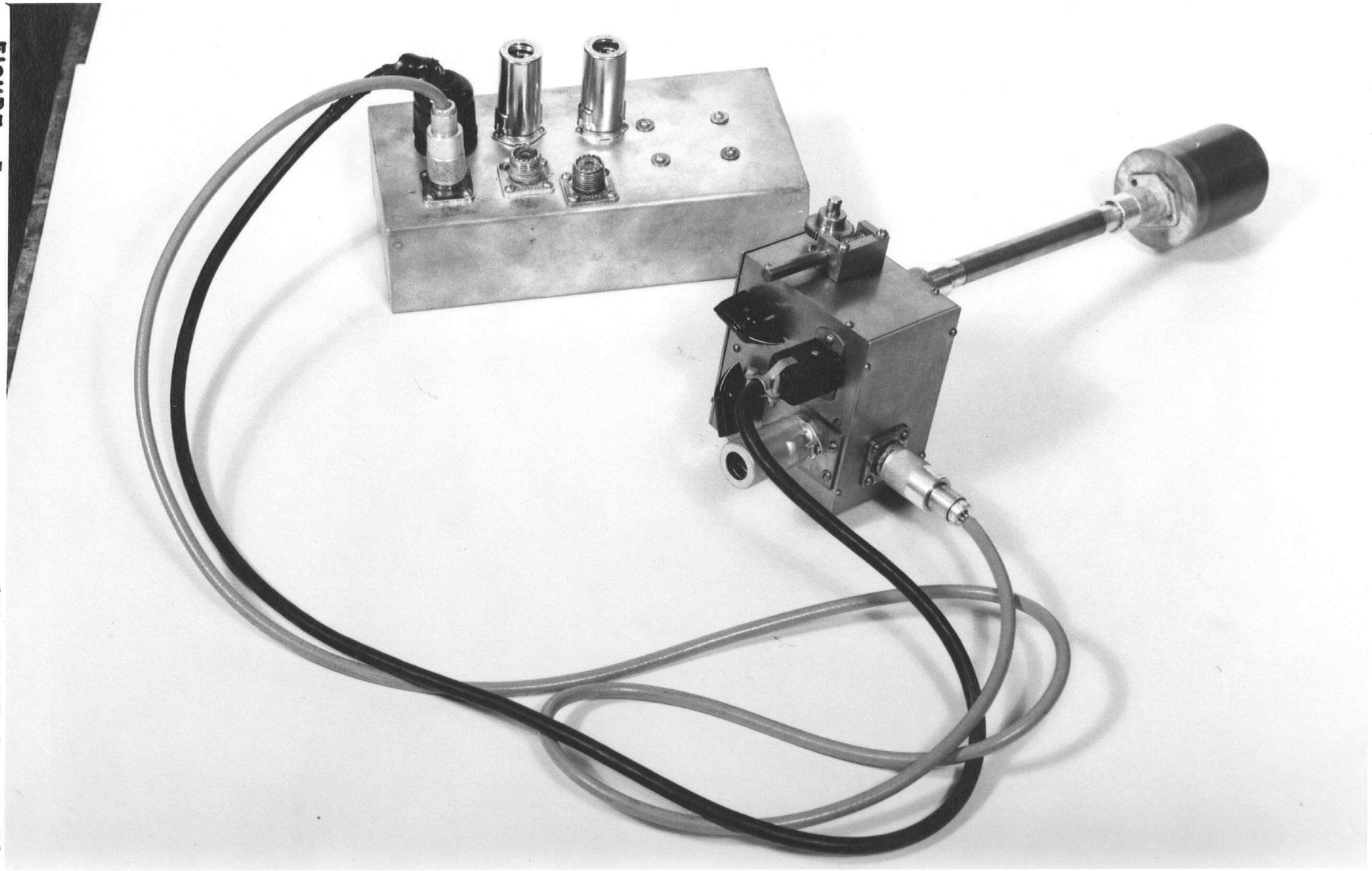

FIGURE 3

LIVINGSTON OSCILLATING DETECTOR & AUDIO AMPLIFIER

TO FACE PAGE 13

nuclear magnetic resonance[11].

It is essential that the oscillation be extremely weak, a condition not easy to attain. As the strength of the oscillation increases the amplitude of the resonance signal decreases. This decrease appears to be due to saturation of the nuclear absorption since the total power that can be absorbed by a small sample is small. For N atoms of spin I at temperature T whose frequency is ν and for which the spin-lattice relaxation time is T_1 the absorbed power P is:

$$P = \frac{2I}{2I+1} \frac{N}{T_1} \frac{(h\nu)^2}{KT}$$

For one cubic centimeter of water at room temperature at 30 megacycles per second, $P = 10^{-9}$ watts[22].

The first oscillating detector constructed involved the Livingston circuit[13]. This apparatus is shown in figures 2 and 3. The design is similar to one used by Hopkins for magnetic field control[14]. The amplifier used with the Livingston oscillator was designed to conform to the available recording apparatus. The Livingston oscillating detector gave good absorption signals for protons in liquids such as water or mineral oil, but very poor signals for protons in solids such as stearic acid. In solids, the optimum oscillation levels are close to the lower limit of stable oscillation. Great difficulty was experienced in lowering the oscillation level of the Livingston oscillator to a point where proton absorption in solids could be properly detected. After several unsuccessful modifications of this design such as increasing the range of the grid bias resistance, and changing the plate voltage, it was decided to build an oscillating detector of different design.

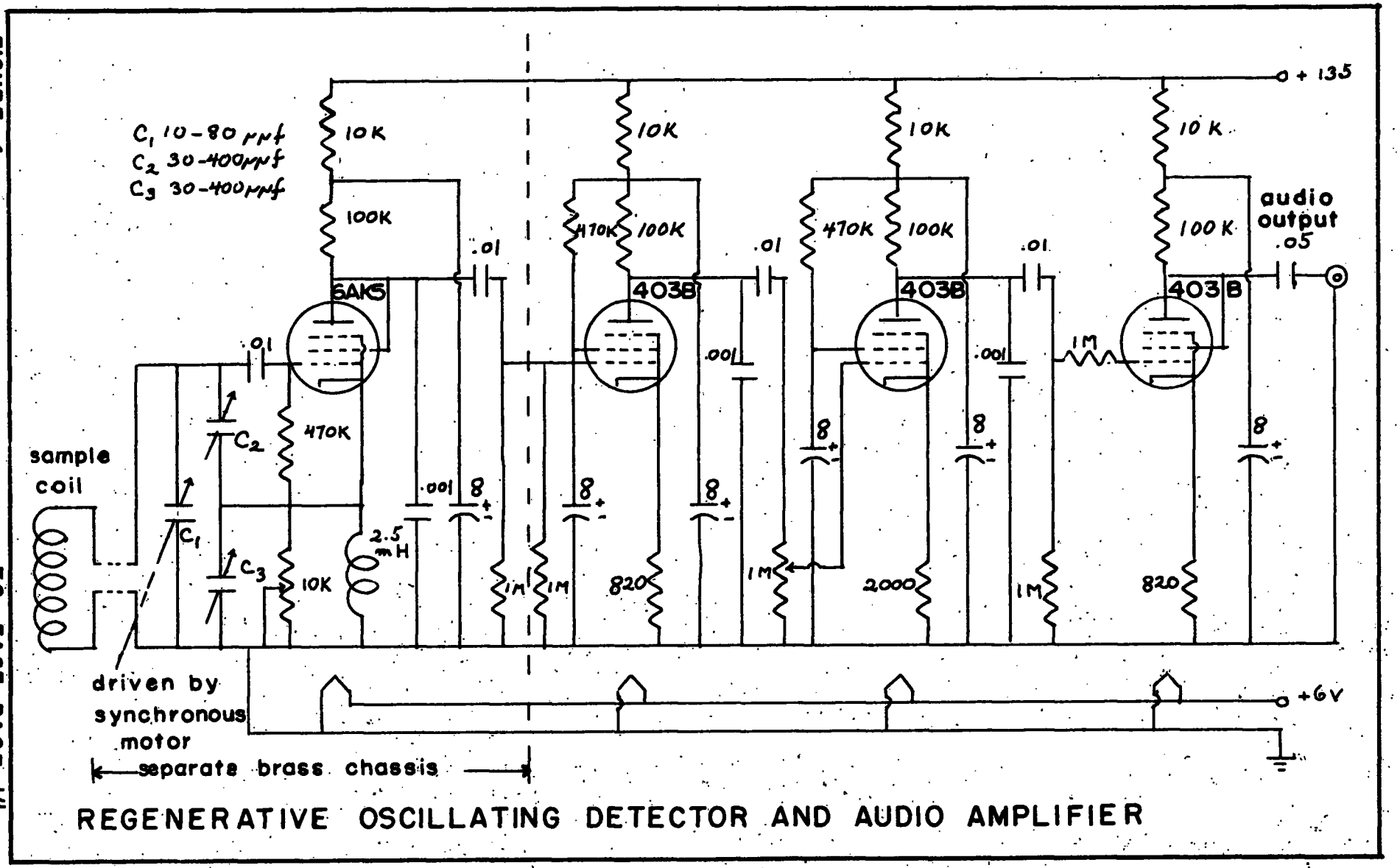

FIGURE 4

REGENERATIVE OSCILLATING DETECTOR AND AUDIO AMPLIFIER

TO FACE PAGE 14

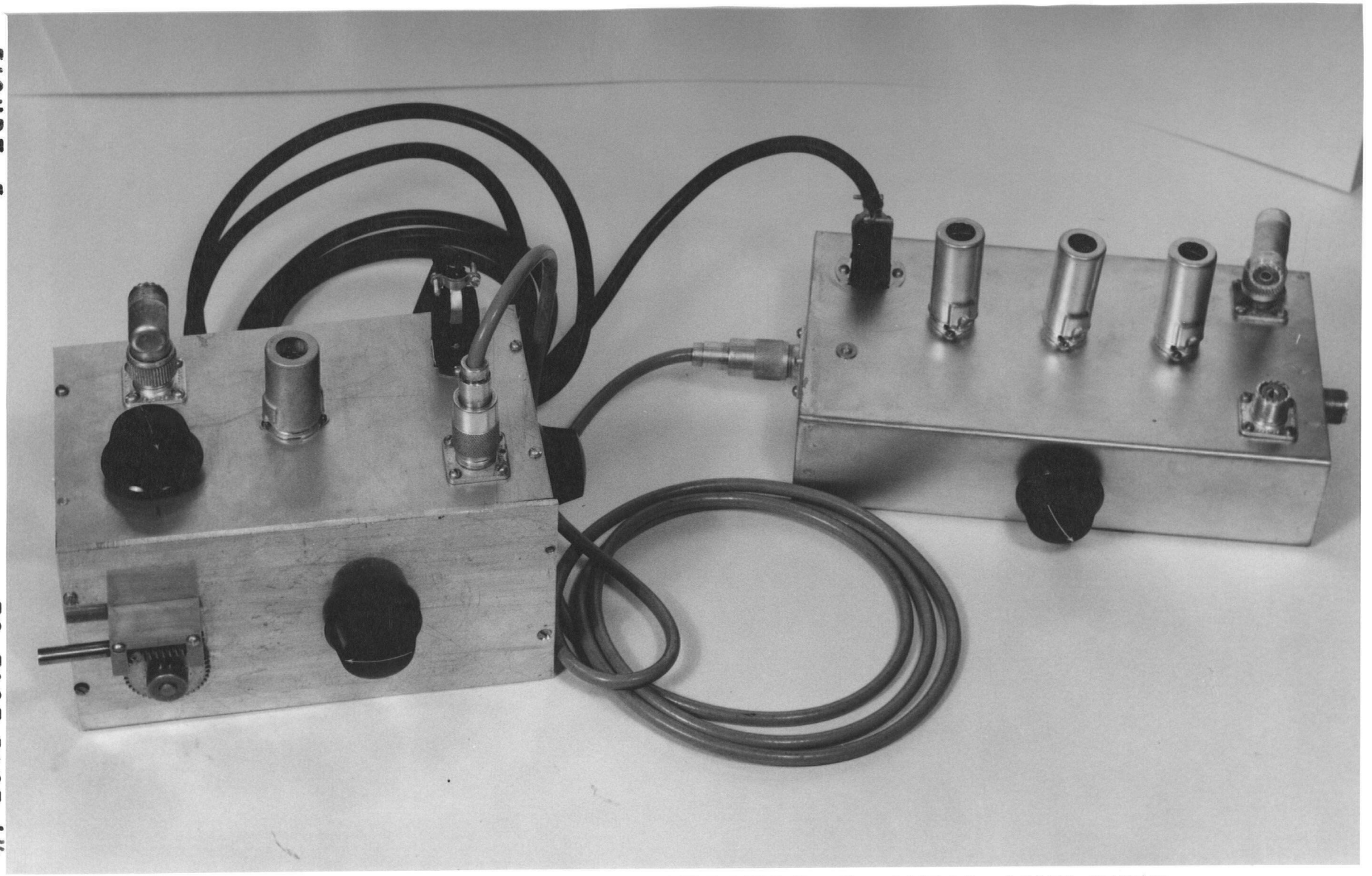

FIGURE 5

REGENERATIVE OSCILLATING DETECTOR & AUDIO AMPLIFIER

TO FACE PAGE 14

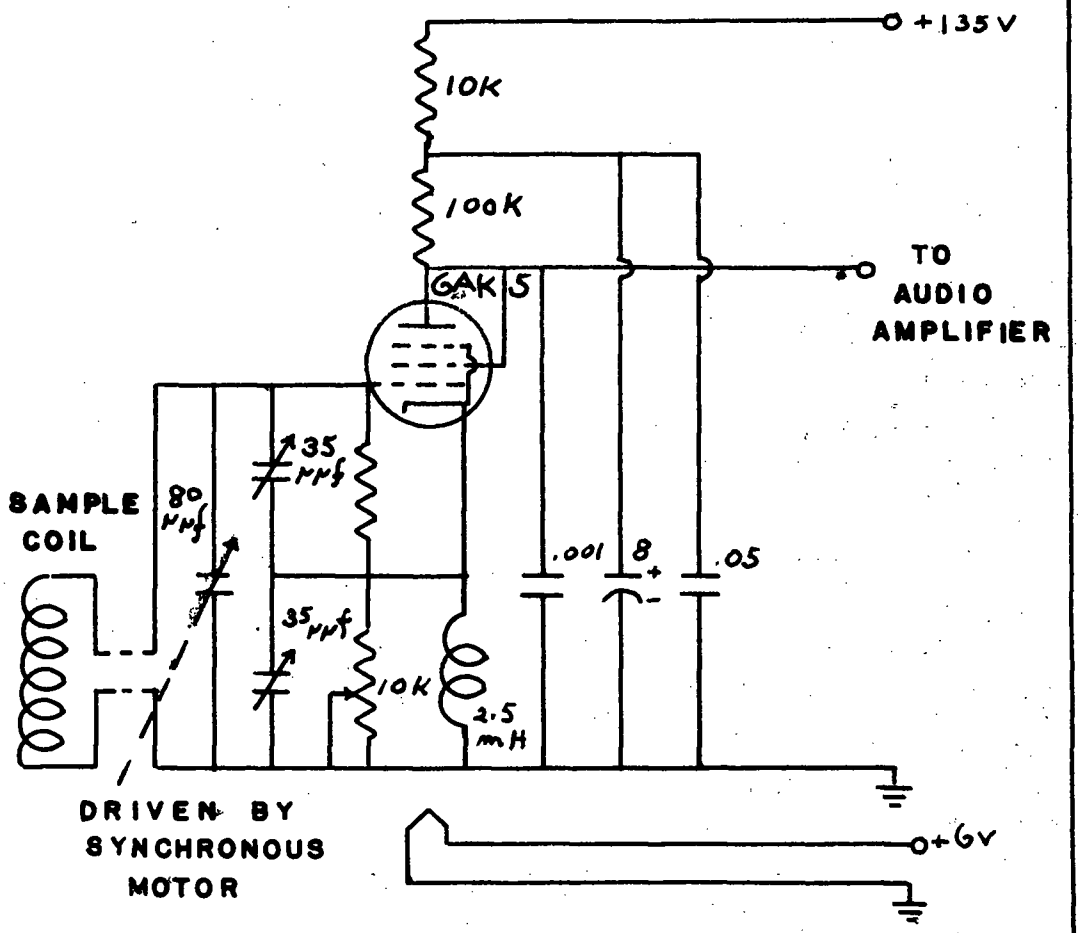

MODIFIED
REGENERATIVE OSCILLATING DETECTOR

FIGURE 6

TO FACE PAGE 14

It is usually necessary to have a special feed-back circuit to stabilize the oscillational level of oscillators operating with variable frequency(19). The Livingston circuit had no such provisions, yet the oscillation level appeared to remain constant over a small frequency range of say 200 kilocycles per second. Since this is greater than the expected line widths a new design need not have the complications mentioned. A suitable circuit has been published by Gutowsky, Meyer and McClure(11). A slightly modified version was built and is shown in figures 4 and 5. The frequency control is provided by the variable air condenser C_1. The frequency range and the general level of oscillation are both controlled by the variable air condensers C_2 and C_3. The variable resistor R_1 provides a finer control of the oscillation level. This instrument, called a regenerative oscillating detector showed proton resonance absorption in both solids and liquids and also gave a much better signal to noise ratio than the Livingston oscillator. A third oscillating detector was then built using the same general design as the second, but incorporating certain refinements shown in figure 6. The main alteration was the replacement of the large 400 micro-micro farad variable condensers C_2 and C_3 with small 35 micro-micro farad ceramic condensers. The apparatus could then be reduced to half its former volume, and a desired higher frequency range could be reached.

The Thermostat.

The arrangement of the thermostat is illustrated in figure 7. The sample is contained in a brass case 6 inches long and 1¼ inches in diameter. From this case extends a tube 20 inches long and one-half inch in diameter which contains the conductor connecting the sample coil to the oscillating detector. This probe was set in a Dewar. The Dewar was about

GENERAL ARRANGEMENT OF APPARATUS

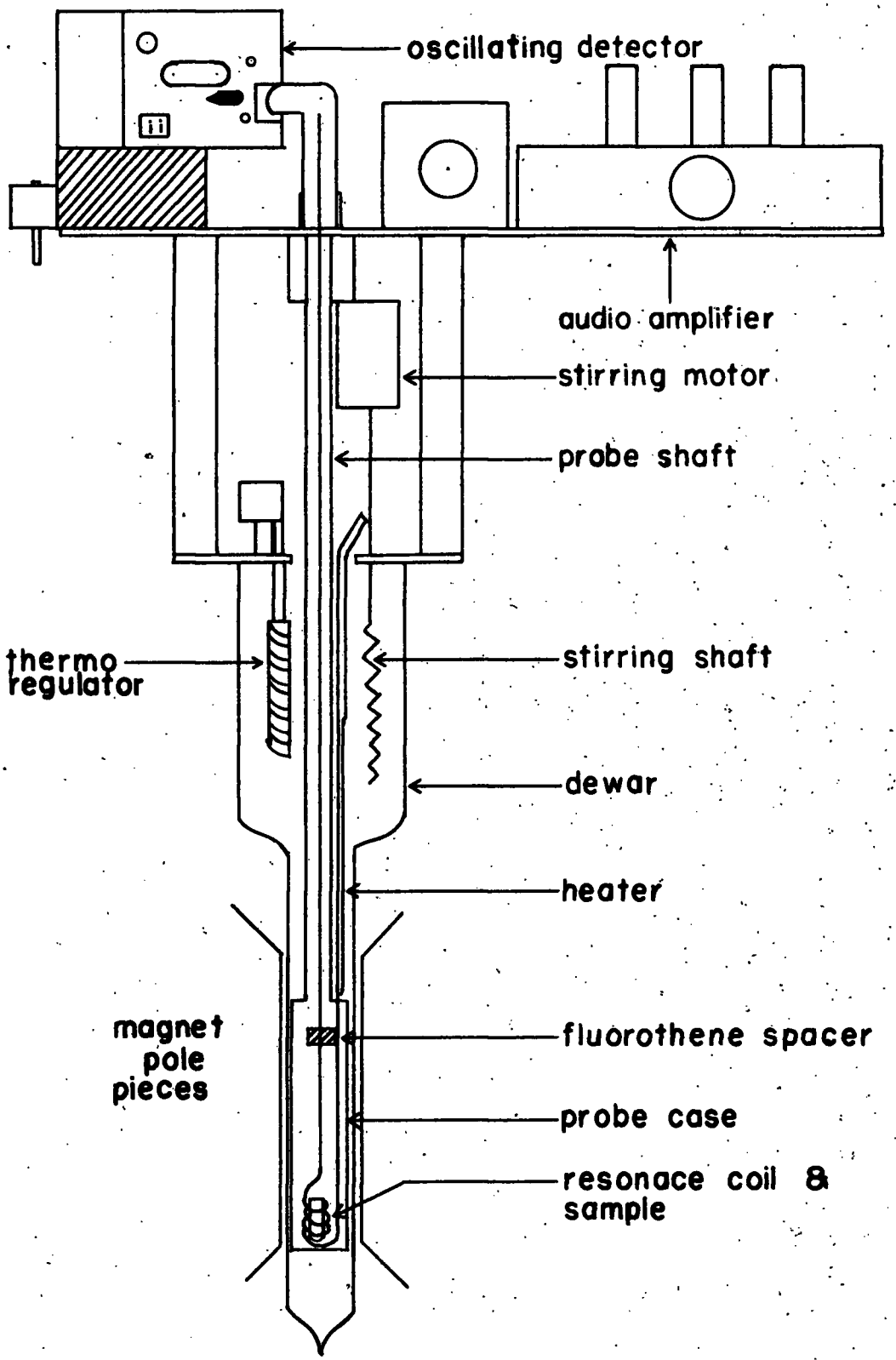

FIGURE 7

TO FACE PAGE 15

1 3/8 inches inside diameter and 1 3/4 inches outside diameter for the bottom 12 inches in order to fit conveniently between the pole pieces of the magnet. For the remaining 8 inches of its length the Dewar widens out to 3 1/2 inches inside diameter to provide a greater volume for a liquid reservoir. A bath of Nujol mineral oil in the Dewar was heated with a Cenco knife type immersion heater. The temperature was controlled with a Cenco De Khotinsky thermoregulator and the liquid was stirred with a crimped aluminum stirring shaft which was rotated with a 6 volt D.C. motor.

The oscillating detector and audio amplifier was set on a large brass plate which in turn rested on a wooden platform above the magnet. The Dewar was secured to the brass plate by means of a plexiglass frame, and by the same means it was held rigid in the magnet gap, clear of both pole pieces.

CHAPTER III EXPERIMENTAL

A. Methods.

Preparation of Sodium Stearate.

The sodium stearate was prepared from Eastman stearic acid which gave a melting point 69-70°C. and a molecular weight of 285. The molecular weight was estimated from the neutralization equivalent which in turn was determined by titrating one gram of stearic acid dissolved in hot alcohol with 0.1 N sodium hydroxide using phenolphthalein as an indicator.

Sodium stearate was prepared by two methods. Stearic acid dissolved in hot 95% ethanol, was titrated with a saturated ethanolic solution of sodium hydroxide to a phenolphthalein end point. Two or three drops extra of the sodium hydroxide solution was added to ensure that all the stearic acid was neutralized. It has been shown that a small excess of sodium salt does not interfere with the phase transitions, whereas excess stearic acid will cause serious changes(27). The sodium stearate was filtered by suction on a Buchner funnel, washed several times with warm ethanol and allowed to dry in air between several leaves of filter paper. The second method is essentially the same as the first except that stearic acid was dissolved in hot absolute ethanol and titrated with a 3% solution of sodium ethoxide in ethanol to a phenolphthalein end point, it was slightly overtitrated as before.

The fluffy sodium stearate crystals contained about 3% water when dry. This could be removed by heating in an oven at 110°C..

Sodium stearate was sealed in melting point tubes and heated in a melting point block. The sodium stearate became translucent at about 130°; at 262° it became transparent and showed a meniscus. These two temperatures agree with phase transition temperatures reported in the literature(30)(32).

A soft glass tube 1/2 inch in diameter and 7 inches long was sealed at one end, and then constricted to 3/16 of an inch in diameter, 1 inch from the sealed end. The result is a bulb 1 inch long and 1/2 in diameter at the bottom of the tube. The open end of the tube was also narrowed sufficiently to fit on a vacuum line. The tube was filled with sodium stearate and melted at 300°C. under vacuum. The fluffy sodium stearate filling the tube melted down to an amount just filling the bulb. The sodium stearate was kept molten for fifteen minutes to remove any water or ethanol and then it was allowed to cool to room temperature. The vacuum system was filled with dry nitrogen and the bulb containing the sample was sealed off. In this manner sodium stearate was made dry and compact, and was protected from oxidation.

Operation of the Thermostat.

The desired temperature was reached by supplying the required power to the knife heater using a variable voltage A.C. power source. This temperature was maintained within about ±1°C. by the thermoregulator and the entire system was allowed to remain at the desired temperature for about one half an hour in order to reach thermal equilibrium. The temperature was measured by mercury-in-glass thermometers which were almost completely immersed in the heating medium. The greater power required to maintain the temperature above say 80°C. also caused some 60 cycle pickup in the oscillating detector which greatly decreased the signal-to-noise ratio. For this reason, the heater power was shut off as soon as the resonance absorption was to be measured. At higher temperatures the error is nearer ±3°C.. The recorded temperature was taken when the resonance absorption signal passed through the Larmor frequency.

Most of the measurements were obtained using Nujol mineral oil as the heating medium. Nujol tended to smoke at temperatures above 150°C. so Fisher bath wax was used for temperatures between 150°C. and 200°C.

Measurement of Resonance Absorption.

The Larmor frequency of protons in a magnetic field of 7070 gauss was found to be 30.1118 Mc/sec.. The resonance absorption line spreads out in a symmetrical manner on both sides of this frequency. The frequency of oscillation of the oscillating detector was found by the communications receiver and was adjusted to within about 100 kc/sec. of the Larmor frequency. The frequency of the oscillating detector was then swept at a uniform speed by a mechanical drive through the frequency region of resonance absorption. The distance on the recorder trace which corresponds to frequency difference was measured by means of a crystal calibrator in the manner described. The width of the resonance absorption line was taken to be the difference in frequency between the peaks on the derivative curve. This frequency difference was then converted into terms of magnetic field by multiplying the frequency by the g factor for protons and $\frac{\mu_0}{k}$. For this case it was found that;

$$\Delta H \text{ (line width in gauss)} = 0.234865\ \Delta\nu \text{ in kc/sec.}$$

The line widths in gauss have been plotted against temperature.

Sources of Error.

The most serious source of error is that involved in determining the exact temperature of the sample. There is some assurance, due to the general reproducibility of line widths, that the difference in temperature between the heating bath and the sample was small, but it could involve a difference of 2-3°C. at higher temperatures.

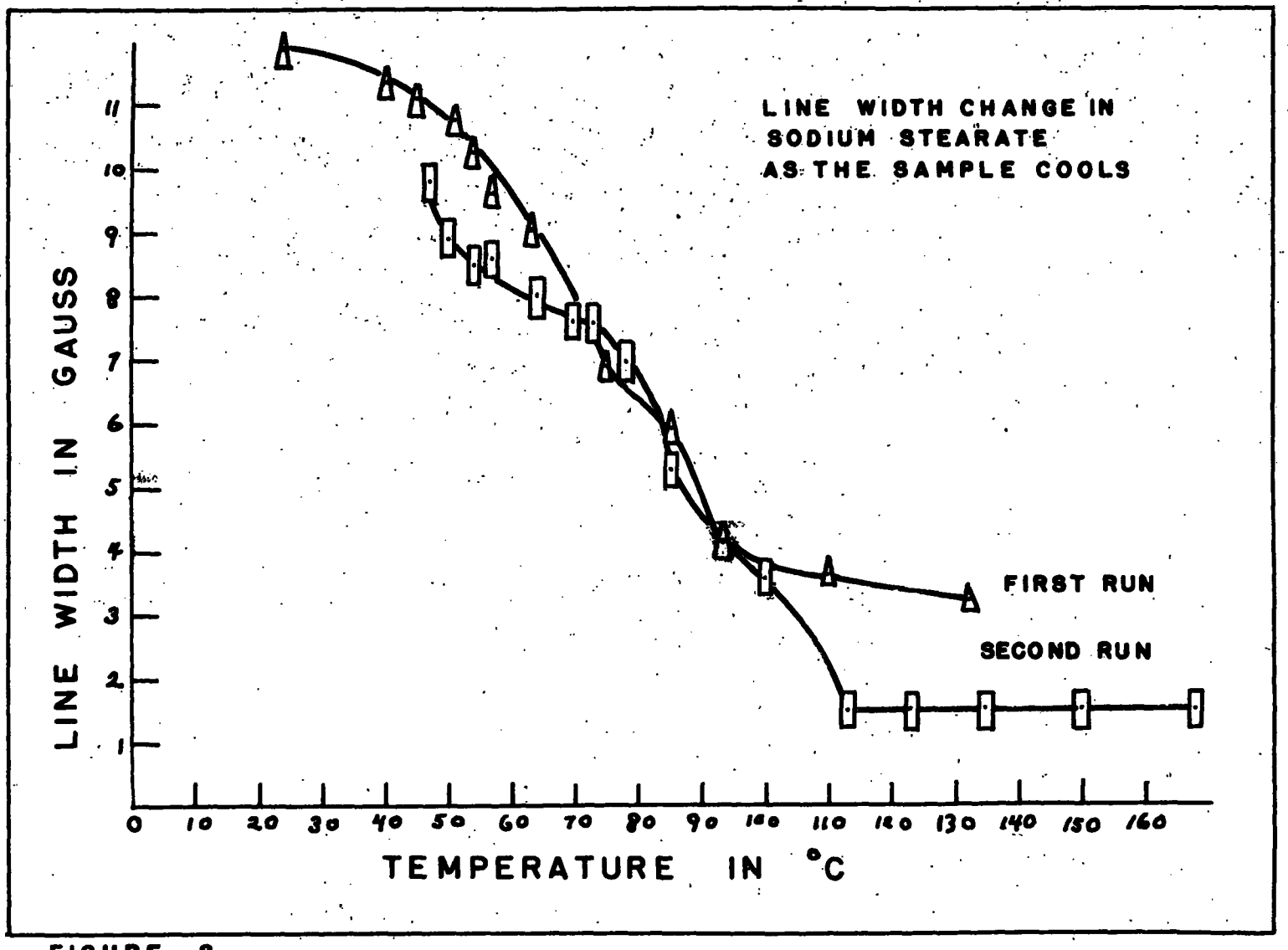

FIGURE 8

TO FACE PAGE 19

Since the actual line width was measured first in terms of distance on the recorder graph, small errors could be introduced due to irregularities in the chart drive. Irregularities in the mechanical drive of the frequency sweep system also produce errors in the position of the signal on the chart although this is minimized to some extent by the system of frequency measurement. At lower temperatures the derivative lines are broader than at higher temperatures and the exact point of maximum deflection on a trace may be difficult to locate. Sometimes the centre of a peak on the derivative curve must be taken as the point of maximum deflection. As a result, the average uncertainty in the line width is about $\pm$ 0.3 gauss.

B. Results.

Phase Transitions in Sodium Stearate.

A preliminary investigation was made on sodium stearate to see if the line width changes in an irregular manner at higher temperatures. One sample was heated to 130°C. and allowed to cool down to room temperature at a rate of approximately one degree centigrade per minute while line width measurements were made. It was then heated to 167°C. and allowed to cool again. The cooling curves in figure 8 indicate that there are rapid changes in the line width at the higher temperatures. The path of the cooling curve depends on the particular temperature to which the sample was originally raised. This hysteresis effect renders the cooling curves of little use for line width investigations.

Line width measurements were made on the same sample at successively higher temperatures in the manner previously described. These measurements were then reproduced using a second sample. The first sample was prepared by titration with sodium hydroxide and the second was prepared

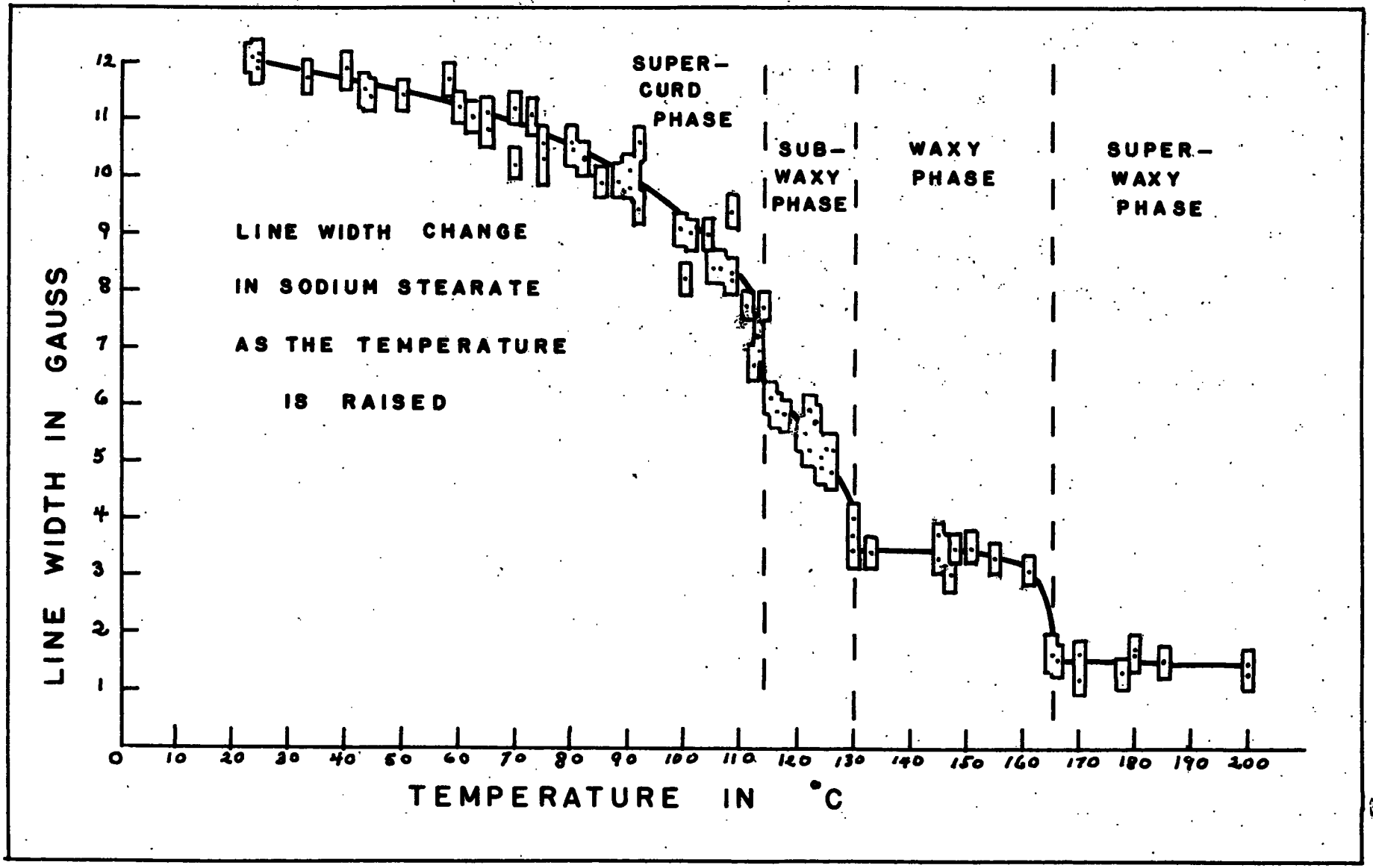

FIGURE 9

TO FACE PAGE 20

by titration with sodium ethoxide. The collected results were plotted against temperature and are shown in figure 9. The resulting curve shows three discontinuities which correspond to phase transitions. These are the supercurd-subwaxy transition at 114°C., the subwaxy-waxy at 130°C. and the waxy-superwaxy transition at 165°C.. The phase transition temperatures fouud are in good agreement with some transition temperatures reported in the literature.

Transition	This Work	Vold(33)	Benton(3)
Supercurd-subwaxy	114°C.	114°C.	-
Subwaxy-waxy	130°C.	134°C.	132°C.
Waxy-superwaxy	165°C.	-	165°C.
Method of Measurement	N.M.R.	Calorimetric	Transmission of Light

The curve in figure 9 shows that the line width decreases evenly from 12 to 10 gauss between room temperature and 90°C.. Above 90°C. the line width decreases more rapidly to about 8 gauss at 110°C.. This more rapid drop might correspond to the supercurd phase reported to begin around 90°C.(30)(33). The supercurd-subwaxy transition at 114°C. is accompanied by a sudden narrowing from 7.5 to 6 gauss. The line width narrows still further from 6 to 3.5 gauss throughout the subwaxy phase. In the waxy phase between 130°C. and 165°C. the line width remains constant at 3.5 gauss. At 165° there is a sudden decrease in line width from 3.5 to 1.5 gauss corresponding to the waxy-superwaxy transition. The line width remains constant at 1.5 gauss throughout the superwaxy phase which ends at 200°C.

Further investigation at higher temperatures were not considered since the line widths found for water and mineral oil were about 1.5 gauss.

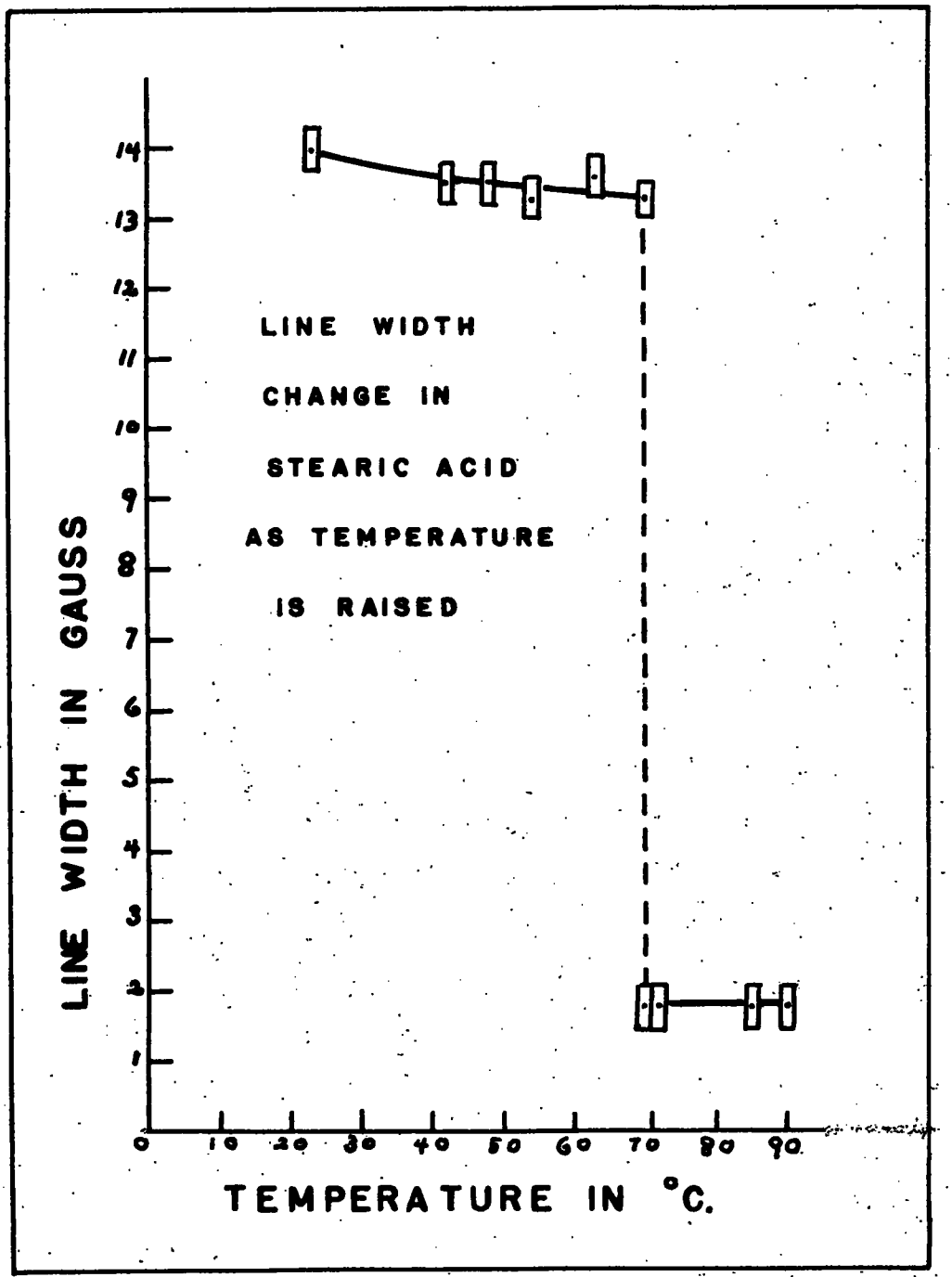

FIGURE 10

TO FACE PAGE 21

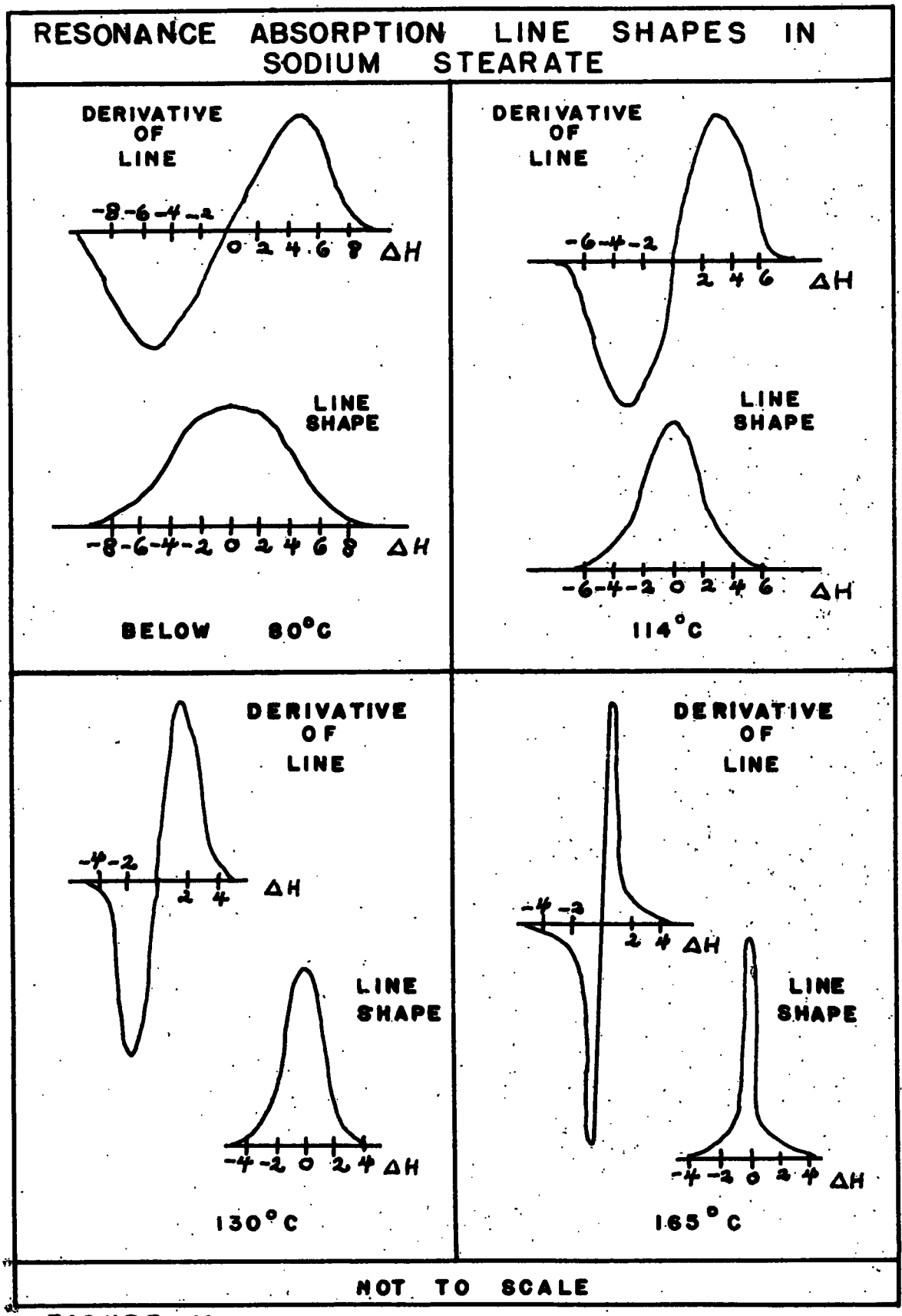

FIGURE 11

TO FACE PAGE 21

An Investigation of Stearic Acid.

Stearic acid was melted into a glass tube of the size used for sodium stearate and line width measurements were made at different temperatures in the manner already described. The resulting line widths were plotted against temperature and are shown in figure 10. The line width remains constant at 13.5 gauss from 24°C. to about 70°C.. At this temperature the stearic acid melts and the line width abruptly decreases to 1.8 gauss.

The Line Shapes of Sodium Stearate.

The line shapes of sodium stearate are shown in figure 11. From 23°C. to about 100°C. the line remains gaussian in character. Above 114°C. the line has a broad base with a narrower peak. The peak becomes narrower still above 130°C. and at 160°C. the line is a narrow spike of liquid line width set on a comparatively broad base.

CHAPTER IV DISCUSSION

Stearic Acid.

The sharp change in line width from 13.5 to 1.8 gauss when stearic acid is melted illustrates the sensitivity of nuclear magnetic resonance to some phase transitions. The spin-spin relaxation time T_2 is inversely proportional to line width if the resonance line always has the same shape[2] . This is true in the case of stearic acid and is approximately so in the case of sodium stearate. In stearic acid the value of T_2 is greatly increased at the melting point, indicating that the effect of the interacting local fields is greatly reduced. It is apparent from this simple illustration that below the melting point the motion of the proton containing groups in stearic acid is greatly hindered by the lattice. There is a large line width due to static interacting fields. However, on melting, the line width narrows greatly, a situation which would indicate that the interacting fields cancel one another out. The proton containing groups, that is, the groups containing hydrogen atoms in the liquid, must therefore be in very rapid motion. The kind of motion that occurs might now be considered. In the case of molten stearic acid, Brownian movement should remove all inter-molecular magnetic interactions and the intra-molecular interactions should be minimized by free rotation about the carbon-carbon bonds.

Sodium Stearate.

Sodium stearate does not give the sharp change in line width that was found for stearic acid because of the mesomorphic phases through which sodium stearate must pass before melting. However, the line width can still be interpreted in terms of molecular motion. The cooling curves of sodium stearate show little sign of phase transitions. This is probably because

the sample was cooled too rapidly and several phases were present simultaneously. The total change in line width will be due to at least two kinds of interactions. As the lattice forms, rotation of bonds in the molecule will be restricted causing intramolecular magnetic interaction. The formation of a more rigid lattice will also pack molecules closer together causing intermolecular magnetic interaction. It has been shown that the effect of interacting magnetic dipoles varies inversely as the cube of the distance between them[12]. The largest contribution to line width would then be the interaction of the protons attached to adjacent carbon atoms in the aliphatic chain. The contribution of other protons further along the chain or in adjacent molecules would be much smaller in comparison.

Since stearic acid melts around 70°C. it can be said that enough energy has been supplied to cause free rotation of proton containing groups in the aliphatic chain portion of sodium stearate. Although most of the narrowing in line width of sodium stearate would be due to bond rotation, the mechanism governing the details of the line width narrowing is probably a change in the lattice which allows rotation to take place. The line width changes in sodium stearate become, in a qualitative sense, a function of the changes in the lattice parameters. This argument is partly supported by the fact that the change in line width from 24°C. to 130°C. follows the dilatometric behaviour of sodium stearate[27].

The line width versus temperature curve in figure 9 shows a gradual loosening of the lattice up to about 80°C.. No special change was found in the vicinity of the genotypical point reported at 70°C.[28]. This may mean that the genotypical point which was found by calorimetric[32] and viscosity measurements[26] might be a rearrangement of the molecules in the lattice that scarcely affects the hindrance to rotation of the proton groups.

The lattice loosens much more rapidly throughout the supercurd phase, which begins above 90°C.. The more abrupt decrease of about 1.5 gauss at 114°C. seems to indicate the end of a trend and perhaps represents the breakdown of the lattice in one dimension. The restrictions on rotation diminish rapidly throughout the subwaxy phase as the lattice continues to loosen. The ends of the hydrocarbon chains are probably receding from each other in directions parallel to the molecular axis.

The waxy phase which extends from 130°C. to 165°C. maintains an almost constant line width. It cannot be said that the lattice is not still loosening or breaking down, however the motion of the proton containing groups must have reached some equilibrium. The lattice has probably altered considerably in a second dimension at 130°C., allowing a slightly restricted rotation of groups. There cannot be much restriction since the line width is only about 3 gauss. Whatever the restriction may be it appears to be completely removed at 165°C. and the line width becomes 1.6 gauss. This is the line width obtained for liquids.

Interpretation of a Line Shape of Sodium Stearate.

When sodium stearate was heated above 165°C., the line became a narrow spike set on a comparatively broad base as shown in figure 11. It has been postulated that the broad base is due to line width broadening resulting from the spin-spin collision of a certain proportion of the protons[21]. This suggests that an organized structure or lattice still exists to some extent above 165°C.. At this temperature the structure or lattice is probably maintained by the strong attraction between the sodium carboxylate ends of the molecule.

Future Work.

Two major phase changes occur in sodium stearate around 200°C. and 265°C. which are attributed to the sodium end of the molecule[9][33]. With some modifications the apparatus used for measuring proton line widths could be used to measure the line widths of sodium. The experiment would be more difficult with sodium nuclei than with protons since the concentration of sodium is relatively small compared to hydrogen, and the sensitivity of sodium nuclei is much less than that of protons[18].

It is not possible to determine the exact mechanism involved in each phase transition by inspection of the line width versus temperature curve. Only a very qualitative estimation can be given. To obtain a more exact description of the mechanism, it is necessary to calculate the theoretical second moment of the line width for sodium stearate under a variety of conditions. For instance, the second moment must first be calculated for a rigid lattice using the known molecular and unit cell parameters[10]. This value is compared to the experimental second moment obtained at low temperatures. Various different conditions of rotation are then calculated in the manner described by Gutowsky and Pake[12] and compared to the experimental results for the various phase transitions[2][23]. Since the spin-lattice relaxation time T_1 may give important contributions to line width change at lower temperatures it must be determined separately. This requires somewhat different apparatus than was used in the present investigation[2]. In such a manner, it is possible to describe the mechanisms of phase transitions with some confidence.

APPENDIX

LINE WIDTHS OF SODIUM STEARATE USED IN FIGURE 9.

1. Sample prepared by neutralizing stearic acid with sodium hydroxide.

Temperature °C.	Line Width in Gauss	Temperature °C.	Line Width in Gauss	Temperature °C.	Line Width in Gauss
24	12.0	80	10.5	113	7.1
24	11.9	80	10.6	116	5.9
24	12.1	82	10.3	118	5.8
33	12.0	85	9.9	122	5.9
33	11.7	88	9.9	124	5.4
41	12.0	90	10.1	126	4.8
43	11.5	92	10.6	130	3.4
50	11.7	92	9.4	130	3.7
58	10.8	99	9.1	133	3.4
60	11.2	100	8.2	145	3.7
65	11.1	101	9.0	145	3.3
65	10.7	104	9.0	147	3.0
70	11.2	105	8.4	155	3.3
70	11.2	106	8.6	165	1.6
73	11.0	108	9.4	170	1.6
75	10.2	108	8.2	185	1.5
75	10.6	111	7.7	200	1.4
80	10.6	113	7.4	200	1.3

2. Sample prepared by neutralizing stearic acid with sodium ethoxide.

Temperature °C.	Line Width in Gauss	Temperature °C.	Line Width in Gauss	Temperature °C.	Line Width in Gauss
23	12.1	122	5.2	151	3.5
44	11.4	123	5.7	161	3.1
62	11.0	124	5.2	165	1.7
91	9.9	125	5.2	165	1.7
108	8.3	126	5.2	166	1.5
112	7.7	130	5.8	178	1.3
114	7.7	130	4.0	180	1.7
115	6.1	148	3.5	180	1.6
121	5.5	149	3.4		

REFERENCES

1. Alpert, N. Phys. Rev., 75, 398 (1949).
2. Andrew, E. and R. Eades, Proc. Roy. Soc. A., 216, 398 (1953).
3. Benton, D., Howe, P., and I. Puddington, Can. J. Chem., 33, 1384 (1955).
4. Bernal, J. and D. Crowfoot, Trans. Faraday Soc., 29, 1032 (1933).
5. Bloembergen, N., Purcell, E. and R. Pound, Phys. Rev., 73, 679 (1948).
6. Buerger, M., Smith, L., De Bretteville, A. and F. Ryer, Proc. Natl. Acad. Sci. U.S., 28, 526 (1942).
7. De Bretteville, A., and J. McBain, J. Chem. Phys., 11, 426 (1943).
8. Doscher, T., and R. Vold, J. Phys. and Colloid Chem., 52, 97 (1948).
9. Gallay, W., and I. Puddington, Can. J. Research B, 21, 202 (1943).
10. Gutowsky, H., Kistiakowsky, G., Pake, G. and E. Purcell, J. Chem. Phys., 17, 972 (1949).
11. Gutowsky, H., Meyer, L., and R. McClure, Rev. Sci. Inst., 24, 644 (1953).
12. Gutowsky, H., and G. Pake, J. Chem. Phys., 18, 162 (1950).
13. Hedgecock, N., Private Communication.
14. Hopkins, N., Rev. Sci. Inst., 20, 401 (1949).
15. Lawrence, A., Trans. Faraday Soc., 34, 660 (1938).
16. McBain, J., Bolduan, O., and S. Ross, J. Am. Chem. Soc., 65, 1873 (1943).
17. McBain, J., Vold, R., and M. Frick, J. Phys. Chem., 44, 1014 (1940).
18. Pake, G., Amer. J. Phys., 18, 438, 473 (1950).
19. Pound, R., and W. Knight, Rev. Sci. Inst., 21, 219 (1950).
20. Powell, B., and I. Puddington, Can. J. Chem., 31, 828 (1953).
21. Purcell, E., Science 107, 433 (1948).
22. Roberts, A., Rev. Sci. Inst., 18, 845 (1947).
23. Rushworth, F., Proc. Roy. Soc. A., 222, 526 (1954).

24. Schuster, N., Rev. Sci. Inst., 22, 254 (1951).

25. Smith, J., Quarterly Reviews, 7, 279 (1953).

26. Southam, F., and I. Puddington, Can. J. Research B. 25, 125 (1947).

27. Stainsby, G., Farnand, R., and I. Puddington, Can. J. Chem., 29, 838 (1951).

28. Thiessen, A., Kleck, J., Gockowinck, H., and J. Stauff, Z. physik. Chem. A., 174, 335 (1935).

29. Thiessen, P., and J. Stauff, Z. physik. Chem. A., 176, 397 (1936).

30. Vold, M., J. Am. Chem. Soc., 63, 160 (1941).

31. Vold, M., Macomber, M., and R. Vold, J. Am. Chem. Soc., 63, 168 (1941).

32. Vold, R., J. Phys. Chem., 49, 315 (1945).

33. Vold, R., J. Am. Chem. Soc., 63, 2915 (1941).

34. Vold, R., Grandine, J., and H. Schott, J. Phys. Chem., 56, 128 (1952).

35. Vold, R., and M. Heldman, J. Phys. and Colloid Chem., 52, 148 (1948).

36. Vorlander, D., Berichte. 43, 3122 (1910).

37. Waterman, H., Ph.D. Thesis, University of British Columbia (1954).

38. Williamson, D., Radiotron Designers Handbook. P. 750 (Radio Corporation of America, Commercial Engineering, Harrison, N. J., 1954).